Wireless Pers Commun (2015) 84:919–933
DOI 10.1007/s11277-015-2668-8

Wideband Power Spectrum Sensing for Cognitive Radios Based on Sub-Nyquist Sampling

Lebing Pan[1,2] · Shiliang Xiao[1,2] · Xiaobing Yuan[1]

Published online: 13 May 2015

Abstract In a cognitive radio system, efficient wideband spectrum estimation is a basic component of dynamic spectrum access. The systems high sampling rate is the main challenge in the frontend. In this paper, wideband power spectrum sensing is studied based on sub-Nyquist sampling instead of signal recovery. Compared to other spectrum sensing methods based on sub-Nyquist sampling, the proposed scheme is suitable for both sparse and nonsparse signals. A low complexity, adaptive resolution frequency averaging scheme is proposed to exploit the cross-power spectrum between the outputs of different channels. Spectrum reconstruction presents only a simple least square without any sparse constraint. The normalized mean square error is computed to demonstrate estimation performance.

Keywords Sub-Nyquist sampling · Cognitive radio · Power spectrum estimation · Wideband sensing

1 Introduction

Alongside booming growth in wireless communication applications, the efficient utilization of spectrum has become a critical consideration for researchers and developers. The cognitive radio (CR) [1] was first proposed for effective spectrum resource usage. This technology allows unlicensed users to access wireless channels when primary users are in an inactive state. Spectrum sensing is an essential functionality to avoid access interference [2, 3]. In a CR system, the wideband frequency spectrum is generally sparse, as not all of the subbands are occupied at the same time; active subbands can be detected by

✉ Lebing Pan
panlb@mail.sim.ac.cn

[1] Key Laboratory of Wireless Sensor Networks, Shanghai Institute of Microsystem and Information Technology, Chinese Academy of Science, Shanghai, China

[2] University of Chinese Academy of Sciences, Beijing, China

compressive sensing [4], known as sub-Nyquist sampling. The method, based on the sub-Nyquist rate, reduces computational burden and memory requirements. The Nyquist rates of wideband signals in a CR system may exceed the specifications of high speed, high-rate analog-to-digital converters (ADCs) [5], which are too power hungry for direct wideband spectrum sensing. However, sub-Nyquist sampling can solve this problem.

Numerous researches refer to acquiring multi-band signal from a rate below the Nyquist sampling rate. Compressive sensing theory is firstly put forward to sense wideband spectrum in [6]. This method reconstructs the wideband spectrum in the first step, then wavelet-based edge detection detects spectral opportunities across the wideband spectrum. A two-step CS scheme was introduced in another study [7] for minimizing sampling rate, where actual sparsity is estimated in the first time slot,then compressed measurements are adjusted in the second slot. Another study explored an adaptive compressive spectrum sensing algorithm for wideband CR [8], in which compressed measurements are adaptively adjusted without any sparsity estimation efforts to improve the throughput. Yet another study [9] developed a multi-rate asynchronous sub-Nyquist sampling (MASS) system to perform wideband spectrum sensing, robust against lack-of-time synchronization and with excellent performance in fading/shadowing scenarios. An efficient collaborative spectrum sensing method with low sample rate was presented by other research [10], employing adopting matching pursuit to detect spectrum holes in a cognitive network. All these studies, however, focused on frequency spectrum estimation or reconstructing original signals. Sparsity order estimation for cognitive radio was investigated in one previous study [11], to provide a general methodology to quantify the minimum number of samples required to estimate sparsity order for compressive spectrum sensing. These works based on sub-Nyquist sampling require an assumption of sparsity in the frequency domain.

In a typical CR system, it is not necessary to recover the original signal but to detect active subbands for dynamic spectrum access. Wideband power spectrum sensing from sub-Nyquist samples no longer requires sparsity assumption. Related works are presented in [12–16]. In [12], wideband power spectrum sensing was considered in the form of inequalities, and only needed a few bits from the nodes in a sensor network. In another work [13], a single-stage frequency-domain sensing technique based on sub-Nyquist sampling was proposed to blindly detect the locations of active subbands. The approach in [14, 15] reconstructed power spectrum of wide-sense stationary signals by exploiting the cross-correlation between the outputs of different channels. A method for finite resolution approximation of power spectrum estimation was proposed in another study [16]. The schemes in [13, 14] based on multi-coset sampling is sensitive to timing jittering. It is difficult to maintain accurate time intervals between channels. The method proposed in [9] introduced an additional estimation error with the high sampling rate of ADCs. In other studies [6–11], methods which used normal compressive sensing reconstruction algorithm with ℓ_1/ℓ_2 norm constraint were proposed, but these usually cause high complexity. In this study, we focus on least square (LS) reconstruction without any sparse constraint. An analog-to-information converter (AIC) [17] is employed with multi-channel parallel architecture, providing a sampler for sparse multi-band signals according to the general concept of random filtering [18]. The sampling framework is similar to the modulated wideband converter (MWC) prototype described in a previous study [19], which is implemented in a wideband receiver in practice.

The rest of this paper is organized as follows. In the second section, an analog signal sub-Nyquist sampling model is described, and the frequency spectrum relationship between samples and the original signal is established. In the third section, we describe the power spectrum relationship between samples and the original signal, which exploits the

cross-power spectrum between the outputs of different channels. The process changes to solve overdetermined equations with a rank condition for reliable estimation. An adaptive resolution frequency averaging (ARFA) scheme is proposed with low complexity in the fourth section. A multiband signal is used for simulation and normalized mean square error (NMSE) is applied to measure the quality of estimation performance. The final section provides a summary and conclusion.

2 Sampling Model

Based on Fig. 1, M branches are employed along with a wide-sense stationary complex-valued analog input $x(t)$. Only considering branch i, $x(t)$ is modulated with a pseudo random signal $p_i(t)$. The signal $p_i(t)$ is a periodic extension of distinct, finite-duration random square waves that share a common period NT, yielded from the piecewise constant function $c_i(t)$. T is the sampling time interval on the Nyquist rate. The length of samples of each branch is L. The average sampling rate is equal to the Nyquist rate multiplied by M/N.

The relation can be expressed as follows:

$$\begin{cases} p_i(t) = c_i(t_0) \quad t = t_0 + lNT,\ 0 \le t_0 < NT, l = 0, 1, \ldots, L \\ c_i(t_0) = c_i[-n] \quad nT \le t_0 < (n+1)T, n = 0, 1, \ldots, N-1 \\ c_i[-n] \in \{-1, 1\} \end{cases} \tag{1}$$

The output of the *i-th* branch with N-fold down-sampling can be represented as

$$\begin{aligned} y_i[k] &= \frac{1}{NT} \int_{kNT}^{(k+1)NT} p_i(t) x(t) dt \\ &= \frac{1}{T} \sum_{n=0}^{N-1} c_i[-n] \int_{(kN+n)T}^{(kN+n+1)T} x(t) dt \\ &= \sum_{n=1-N}^{0} c_i[n] x[kN - n] \\ &= s_i[kN] \end{aligned} \tag{2}$$

There is a key operation of $c_i(t_0) = c_i[-n]$ in (1). The output of each branch can be regarded as the N-fold down-sampling of $s_i[n] = c_i[n] * x[n]$ from (2), where $*$ represents the linear convolution operator.

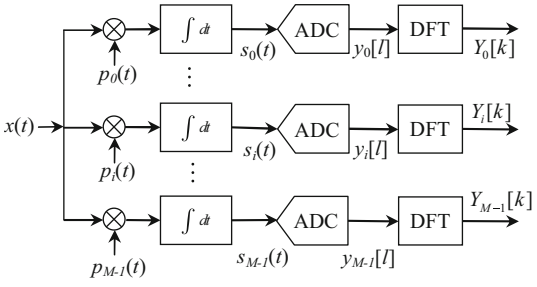

Fig. 1 Multi-channel parallel AIC sub-Nyquist sampling framework

The output is equal to the N-fold down-sampling from $s_i'[n]$. $s_i'[n] = c_i'[n] \circledast x[n]$, where $\circledast$ is the circular convolution operator. $\mathbf{c}_i' = [\mathbf{c}_i, \mathbf{0}_{1\times(L-1)N}]$ (where $\mathbf{0}$ is zero matrix, $\mathbf{c}_i = [c_i[0], c_i[1], \ldots, c_i[N-1]]$). The length of $c_i'[n]$ is identical to $x[n]$. Then following is then obtained

$$\begin{aligned} y_i[l] &= s_i'[(l+1)N-1] \\ &= \frac{1}{LN}\sum_{k=0}^{LN-1} S_i'[k] e^{j\frac{2\pi}{LN}k[(l+1)N-1]} \quad l = 0, 1, \ldots, L-1 \end{aligned} \tag{3}$$

where $S_i'[k]$ is the LN-points discrete Fourier transform (DFT) of $s_i'[n]$. In the frequency domain, with the circular convolution theorem:

$$S_i'[k] = C_i'[k]X[k] \tag{4}$$

where $C_i'[k]$ is LN-points DFT of $c_i'[n]$, and $X[k]$ is the LN-points DFT of $x[n]$. We then can have the L-points DFT of $y_i[l]$:

$$\begin{aligned} Y_i[k] &= \frac{1}{LN}\sum_{l=0}^{L-1} y_i[l] e^{-j\frac{2\pi}{L}lk} \\ &= \frac{1}{LN}\sum_{l=0}^{L-1}\left[\sum_{m=0}^{LN-1} X[m]C_i'[m] e^{j\frac{2\pi}{LN}m[(l+1)N-1]}\right] e^{-j\frac{2\pi}{L}lk} \\ &= \frac{1}{N}\sum_{m} X[m]C_i'[m] e^{j\frac{2\pi}{LN}m(N-1)} \frac{1}{L}\sum_{l=0}^{L-1} e^{j\frac{2\pi}{L}(m-k)l} \end{aligned} \tag{5}$$

It is obvious that

$$\frac{1}{L}\sum_{l=0}^{L-1} e^{j\frac{2\pi}{L}(m-k)l} = \begin{cases} 1 & m-k = 0, L, 2L, \ldots, (N-1)L \\ 0 & others \end{cases} \tag{6}$$

From (5–6), we can have

$$\begin{aligned} Y_i[k] &= \frac{1}{N}\sum_{n=0}^{N-1} X[nL+k]C_i'[nL+k] e^{j\frac{2\pi}{LN}(nL+k)(N-1)} \\ &= \frac{1}{N}\sum_{n=0}^{N-1} X[nL+k]C_i''[nL+k] \end{aligned} \tag{7}$$

where $C_i''[nL+k] = C_i'[nL+k]e^{j\frac{2\pi}{LN}(nL+k)(N-1)}$. From (7), the multi-branch output can be written in matrix form as follows:

$$\mathbf{y}[k] = \frac{1}{N}\mathbf{C}''[k]\mathbf{x}[k] \quad k = 0, 1, \ldots, L-1 \tag{8}$$

where the relation is

$$\begin{aligned}
\mathbf{y}[k] &= [Y_0[k], Y_1[k], \ldots, Y_{M-1}[k]]^T \\
\mathbf{x}[k] &= [X[k], X[L+k], \ldots, X[L(N-1)+k]^T \\
\mathbf{C}''[k] &= \begin{bmatrix} C''_0[k] & C''_0[L+k] & \cdots & C''_0[L(N-1)+k] \\ C''_1[k] & C''_1[L+k] & \cdots & C''_1[L(N-1)+k] \\ \vdots & \vdots & \vdots & \vdots \\ C''_{M-1}[k] & C''_{M-1}[L+k] & \cdots & C''_{M-1}[L(N-1)+k] \end{bmatrix}
\end{aligned} \tag{9}$$

From (8), we finally obtain

$$\begin{bmatrix} \mathbf{y}[0] \\ \mathbf{y}[1] \\ \vdots \\ \mathbf{y}[L-1] \end{bmatrix} = \frac{1}{N} \begin{bmatrix} \mathbf{C}''[0] & & \mathbf{0} \\ & \mathbf{C}''[1] & \\ & \ddots & \\ \mathbf{0} & & \mathbf{C}''[L-1] \end{bmatrix} \begin{bmatrix} \mathbf{x}[0] \\ \mathbf{x}[1] \\ \vdots \\ \mathbf{x}[L-1] \end{bmatrix} \tag{10}$$

The frequency spectrum of $x[n]$ is expressed as:

$$\mathbf{x} = vec\{[\mathbf{x}[0]^T, \mathbf{x}[1]^T, \ldots, \mathbf{x}[L-1]^T]\} \tag{11}$$

where vec{.} stacks all columns of a matrix into a vector. We cannot directly obtain $\mathbf{x}[k]$ from (8) because $\mathbf{C}''[k]$ is not a full column rank matrix (where $M < N$).

3 Wideband Power Spectrum Estimation

In a CR system, spectrum sensing detects the active subbands rather than recovering the original signal. In this section, we estimate the power spectrum of wide-sense stationary analog input to detect the active bands. The signal exhibiting cyclostationary has an auto-correlation function $R_x(t, \tau) = \mathrm{E}\{x(t)x^*(t+\tau)$, which is periodic in the time domain with a period T_0

$$R_x(t + T_0, \tau) = R_x(t, \tau) \tag{12}$$

The power spectrum of $x[n]$ is given as

$$P_x[k] = X[k]X^*[k] \tag{13}$$

where * denotes conjugation. The cross-power spectrum of $y_i[k]$ and $y_j[k]$ can be written as

$$P_{y_{i,j}}[k] = Y_i[k]Y_j^*[k] \tag{14}$$

The cross-power spectrum of $c'_i[n]$ and $c'_j[n]$ can be computed offline as

$$P_{c_{i,j}}[k] = C'_i[k]C'^*_j[k] \tag{15}$$

It is obvious that $C'_i[k]C'^*_j[k] = C''_i[k]C''^*_j[k]$, then a relation similar to (8) is drawn

$$\mathbf{p}_y[k] = \frac{1}{N^2}\mathbf{P}_C[k]\mathbf{p}_x[k] \quad k = 1, 2, \ldots, L \tag{16}$$

where the relation is

$$\begin{aligned}
\mathbf{p}_y[k] &= [P_{y_{0,0}}[k], P_{y_{0,1}}[k] \ldots, P_{y_{i,j}}[k], \ldots]^T \\
\mathbf{p}_x[k] &= [P_x[k], P_x[L+k], \ldots, P_x[L(N-1)+k]]^T \\
\mathbf{P}_C[k] &= \begin{bmatrix} P_{c_{0,0}}[k] & P_{c_{0,0}}[L+k] & \cdots & P_{c_{0,0}}[L(N-1)+k] \\ P_{c_{0,1}}[k] & P_{c_{0,1}}[L+k] & \cdots & P_{c_{0,1}}[L(N-1)+k] \\ \vdots & \vdots & \vdots & \vdots \\ P_{c_{0,0}}[k] & P_{c_{0,0}}[L+k] & \cdots & P_{c_{i,j}}[L(N-1)+k] \end{bmatrix}
\end{aligned} \tag{17}$$

$\mathbf{P}_C[k]$ is a $M^2 \times N$ deterministic matrix. From (16), we finally obtain

$$\begin{bmatrix} \mathbf{p}_y[0] \\ \mathbf{p}_y[1] \\ \vdots \\ \mathbf{p}_y[L-1] \end{bmatrix} = \frac{1}{N^2} \begin{bmatrix} \mathbf{P}_C[0] & & \mathbf{0} \\ & \mathbf{P}_C[1] & \\ & \ddots & \\ \mathbf{0} & & \mathbf{P}_C[L-1] \end{bmatrix} \begin{bmatrix} \mathbf{p}_x[0] \\ \mathbf{p}_x[1] \\ \vdots \\ \mathbf{p}_x[L-1] \end{bmatrix} \tag{18}$$

The power spectrum of $x[n]$ is written as

$$\mathbf{p}_x = vec\{[\ldots, \mathbf{p}_x[k], \ldots]\} \quad k = 0, 1, \ldots, L-1 \tag{19}$$

While the compressive sampling matrix $\mathbf{C}$ is given as

$$\mathbf{C}_{M \times N} = \left[\mathbf{c}_0^T, \mathbf{c}_1^T, \ldots \mathbf{c}_{M-1}^T\right]^T \tag{20}$$

The rank of $\mathbf{C}$ is $r_C = rank(\mathbf{C})$ (where $rank(\mathbf{X})$ denotes the rank of matrix $\mathbf{X}$). When $M \ll N$, the value of r_C is usually equal to M.

Proposition *If $M^2 \geq N$, $\mathbf{P}_C[k]$ is a full column rank matrix.*

Proof From (15), the element in $\mathbf{P}_C[k]$ is given

$$\begin{aligned}
P_{c_{i,j}}[nL+k] &= C_i'[nL+k] C_j'^*[nL+k] \\
&= \left(\sum_{m=0}^{N-1} c_i[m] e^{-j\frac{2\pi}{LN}m(nL+k)}\right) \times \left(\sum_{m=0}^{N-1} c_j[m] e^{j\frac{2\pi}{LN}m(nL+k)}\right) \\
&= c_i \mathbf{f}_{nL+k}^T \mathbf{f}_{nL+k}^* c_j^T \\
&= c_i \mathbf{F}_{nL+k} c_j^T
\end{aligned} \tag{21}$$

where $\mathbf{f}_{nL+k} = [1, W^{(nL+k)}, \ldots, W^{(N-1)(nL+k)}]$ is the Fourier transformation vector and $W = e^{-j\frac{2\pi}{LN}}$ is an exponential factor. $\mathbf{F}_{nL+k} = \mathbf{f}_{nL+k}^T \mathbf{f}_{nL+k}^*$. From (17) and (20), we can have

$$\mathbf{p}_{c_{i,j}}[k] = \mathbf{C}_{A_i} \mathbf{F}_D \mathbf{c}_{B_j} \tag{22}$$

where $\mathbf{C}_{A_i} = \mathbf{U}_N \otimes \mathbf{c}_i$ ($\otimes$ denotes Kronecker product, $\mathbf{U}_N$ is a unit matrix with size N), $\mathbf{c}_{B_j} = [\mathbf{c}_j, \mathbf{c}_j, \ldots, \mathbf{c}_j]^T$ and $\mathbf{F}_D = \mathrm{diag}(\mathbf{F}_k, \mathbf{F}_{L+k}, \ldots, \mathbf{F}_{(N-1)L+k})$. $\mathrm{diag}(\mathbf{X}_1, \mathbf{X}_2, \ldots, \mathbf{X}_g)$ denotes a block diagonal matrix with principal diagonal blocks $\mathbf{X}_1, \mathbf{X}_2, \ldots, \mathbf{X}_g$. $\mathbf{c}_{B_j}$ is a vector containing N groups of $\mathbf{c}_j$. From (17) and (22), it is given

$$\mathbf{P}_C[k] = \mathbf{C}_B \mathbf{F} \mathbf{C}_A \tag{23}$$

where $\mathbf{C}_A = [\mathbf{C}_{A_0}, \mathbf{C}_{A_1}, \ldots \mathbf{C}_{A_{M-1}}]^T$, $\mathbf{C}_B = U_N \otimes \mathbf{C}_{B_0}$, $\mathbf{C}_{B_0} = [\mathbf{c}_{B_0}, \mathbf{c}_{B_1} \ldots \mathbf{c}_{B_{M-1}}]^T$ and $\mathbf{F} = \mathbf{U}_M \otimes \mathbf{F}_D^T$ ($\mathbf{U}_M$ is a unit matrix with size M).

$\mathbf{F}$ is a block diagonal matrix with the $M \times N$ nonzero blocks. $\mathbf{C}_A$ is a matrix with M nonzero block diagonal matrix arranged in a column. While assuming $r_C{=}M$, each block $\mathbf{C}_{A_i}$ in $\mathbf{C}_A$ is independent (which means that each block matrix $\mathbf{C}_{A_i}$ cannot have a linear expression with other blocks). $\mathbf{C}_B$ is a block diagonal matrix with M blocks, each block is equal to $\mathbf{C}_{B_0}$, and $rank(\mathbf{C}_{B_0}) = rank(\mathbf{C}) = M$. Thus, the rank of $\mathbf{P}_C[k]$ is given

$$rank(\mathbf{P}_C[k]) = \min\{M^2, N\} \tag{24}$$

where min $\{.\}$ denotes the smaller element of the two numbers. From (24), $\mathbf{P}_C[k]$ has full column rank when

$$M^2 \geq N \tag{25}$$

Because $\mathbf{C}_{M\times N}$ is a random matrix, it is easy to design according to the requirements of (25). If $\mathbf{P}_C[k]$ is a full column rank matrix, (15) is solvable using LS. Denoting its pseudo inverse as $\mathbf{P}_C^{\dagger}[k]$, $\widehat{\mathbf{p}}_x[k]$ is attained as the estimation of $\mathbf{p}_x[k]$ without any additional constraints.

$$\frac{1}{N^2}\widehat{\mathbf{p}}_x[k] = \mathbf{P}_C^{\dagger}[k]\mathbf{p}_y[k] \tag{26}$$

□

4 Adaptive Resolution Frequency Averaging (ARFA) Method

The modulated signal in a communication system is wide-sense stationary. This underlying stationary assumption allows us to use the frequency averaging method. This section introduces three methods based on frequency averaging in effort to decrease the envelope fluctuation.

Definition The length of $\widehat{\mathbf{p}}_x[k]$ is LN. The length of $\widehat{\mathbf{p}}_x[k']$ computed by frequency averaging is $L'N$ and $Z = L/L'$, where L' is the adaptive resolution factor. The spectrum averaging of the original signal is expressed as

$$X[k'] = \frac{1}{Z}\sum_{k=k'Z}^{(k'+1)Z-1} X[k] \quad k' = 0, 1, \ldots, L'N - 1 \tag{27}$$

The reference power spectrum is written as

$$\mathbf{P}_x[k'] = \mathbf{X}[k']\mathbf{X}^*[k'] \tag{28}$$

The resolution of $\mathbf{p}_x[k']$ is $1/L'N$.

The first of the three methods is the direct frequency averaging method (DFAM). After obtaining the estimation results of power spectrum with (26), DFAM computes the average value of the segments divided from the estimation. The number of segments is $L'N$. The results are provided by

$$\widehat{\mathbf{p}}_x[k'] = \frac{1}{Z}\sum_{k=k'Z}^{(k'+1)Z-1} \widehat{\mathbf{p}}_x[k] \quad k' = 0, 1, \ldots, L'N - 1 \tag{29}$$

The second method is the periodogram averaging method (PAM). The periodogram method [20] is a basic power spectrum estimation method that decreases envelope

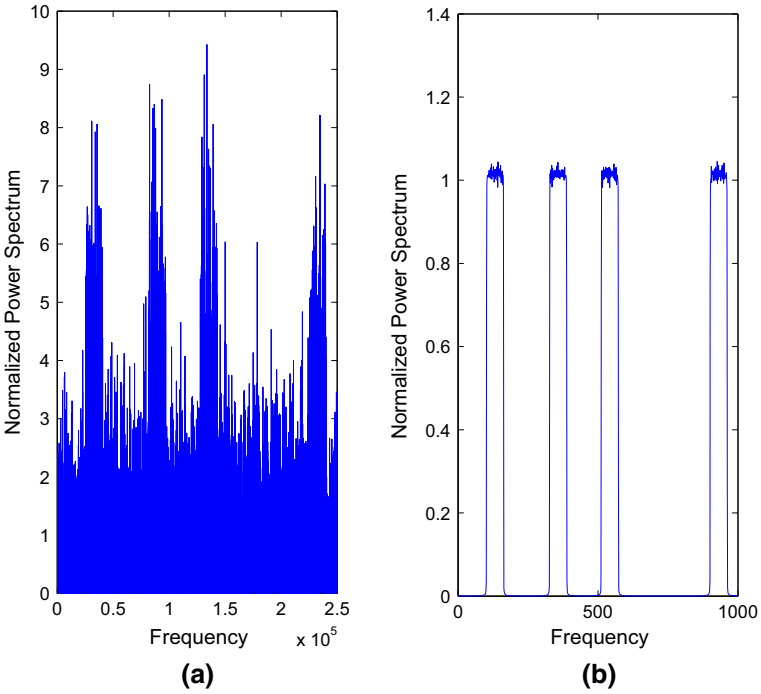

Fig. 2 L = 1000, N = 256, Compression rate = 0.25. **a** Original power spectrum estimation. **b** Reference power spectrum, $L' = 4$

fluctuation. PAM first divides the signal into $L'N$ segments, then the power spectrum of each segment is estimated by (26) in turn. The output is the average value of all segments, expressed as follows:

$$\widehat{\mathbf{p}}_x[k'] = \frac{1}{Z}\sum_{j=0}^{Z-1} \widehat{\mathbf{p}}_{x_j}[k'] \quad k' = 0, 1, \ldots, L'N - 1 \tag{30}$$

where j is segment index. In practice, it is difficult to reconstruct $\mathbf{p}_x[k]$ $(k = 1, 2, \ldots, L)$ when the value of L is large. An adaptive resolution frequency averaging (ARFA) method is proposed. ARFA first divides the frequency spectrum $\mathbf{Y}[k]$ into $L'N$ segments, then the average value of the frequency spectrum of all segments is computed. Equation (26) provides the estimation results. The corresponding operation is given

$$\begin{aligned} \mathbf{c}_i'[n] &= [\, \mathbf{c}_i[n] \,,\, \mathbf{0}_{1\times(L'-1)N}] \\ Y_i[k'] &= \frac{1}{Z}\sum_{k=k'Z}^{(k'+1)Z-1} Y_i[k] \\ P_{y_{i,j}}[k'] &= Y_i[k']Y_j^*[k'] \quad k' = 0, 1, \ldots, L' - 1 \end{aligned} \tag{31}$$

(7) is rewritten in averaging approximate form as

$$
\begin{aligned}
Y_i[k'] &= \frac{1}{N}\sum_{n=0}^{N-1}\left(\frac{1}{Z}\sum_{k=nL+k'Z}^{nL+(k'+1)Z-1} X[k]\right)\left(\frac{1}{Z}\sum_{k=k'Z}^{(k'+1)Z-1} C_i''[k]\right) \\
&= \frac{1}{N}\sum_{n=0}^{N-1} X[nL'+k']C_i'[nL'+k'])
\end{aligned}
\tag{32}
$$

where C_i' is the $L'N$-points DFT of c_i' in (32). Equation (26) is reexpressed as

$$
\frac{1}{N^2}\widehat{\mathbf{p}}_x[k'] = \mathbf{P}_C^{\dagger}[k']\mathbf{p}_Y[k'] \quad k' = 0, 1, \ldots, L'-1 \tag{33}
$$

There are only L' group equations to be solved by (33) for ARFA, while DFAM and PAM methods need to solve L group equations with (26). The frequency resolution of $\widehat{\mathbf{p}}_x[k']$ is $\frac{1}{L'N}$.

5 Simulation Results

This section provides some simulations that to demonstrate the performance of power spectrum estimation with the ARFA method. The multi-band orthogonal frequency division multiplexing (OFDM) signal is selected as the analog input, that investigated as a candidate transmission technology for CR [21, 22]. The spectrum shape of each subband is rectangular.

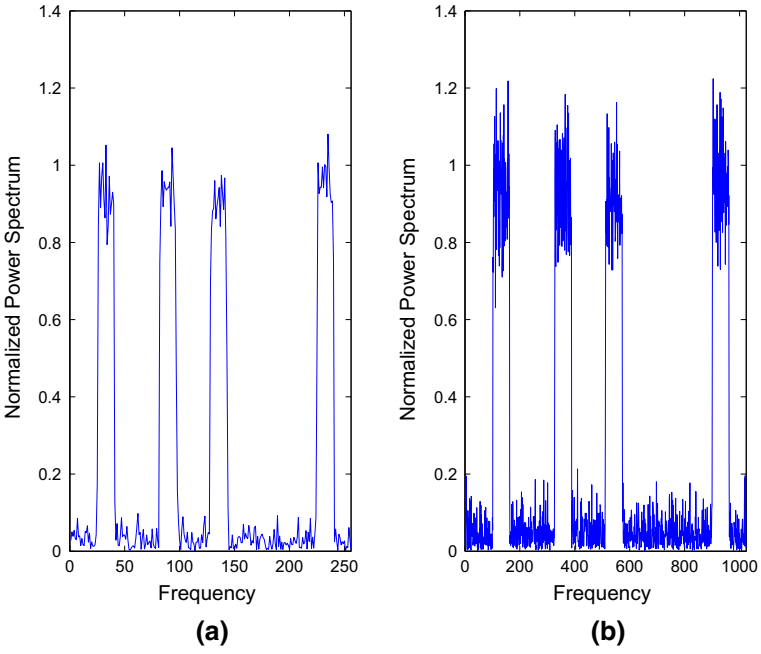

Fig. 3 Power spectrum estimation with different frequency resolution, L = 1000, N = 256, **a** $L' = 1$, **b** $L' = 4$

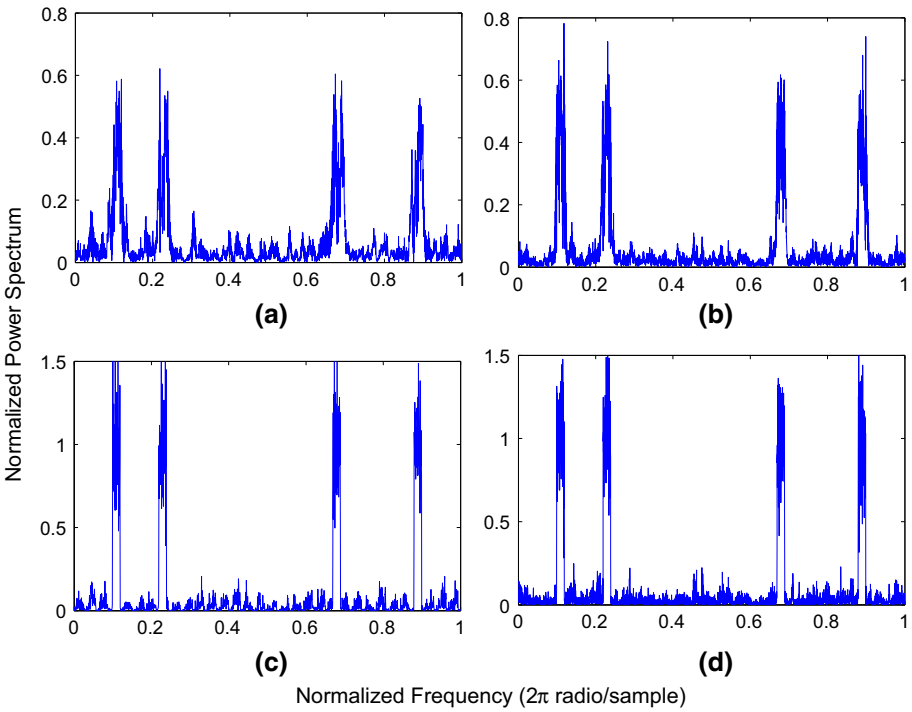

Fig. 4 Power spectrum estimation from compressive samples. **a**, **c** $M = 16, N = 32$. **b**, **d** $M = 32, N = 64$. **a**, **b** PSBS method. **c**, **d** ARFA method

Figure 2a is the estimation result computed by (26). The reference power spectrum in Figure 2b was computed by (27–28). Figure 3 illustrates the estimation performance versus frequency resolution. High frequency resolution estimation introduces envelope fluctuation. Figure 3a demonstrates a special case of $L = 1$, which is only needed to solve one equation.

The number of total subcarriers is N_c ($N_c = 2048$ in the following test), which indicates signal bandwidth. The number of active subbands is N_b. Figure 4 shows a test result with noise-free input. The number of active bands is $N_b = 4$, $L = 1000$, and each subband employs 40 subcarriers. In Fig. 4a, c, $M = 16$, $N = 32$. In Fig. 4b, d, $M = 32$, $N = 64$. The adaptive resolution factor is $L' = 16$ in Fig. 4c, d.

The PSBS method proposed in [15] introduces estimation error, as shown in Fig. 4a, b. The estimation error increases when the value of N is smaller (Fig. 4a, b). However, this modification barely affects estimation performance with the ARFA method in Fig. 4c, d.

NMSE is used to measure the quality between power spectrum estimation results and the reference power spectrum. It is defined as

$$\text{NMSE} := \mathbb{E}\left[\frac{\left\|\hat{P}_x[i] - P_r[i]\right\|^2}{\left\|P_r[i]\right\|^2}\right] \tag{34}$$

where P_r is the reference power spectrum, expressed as

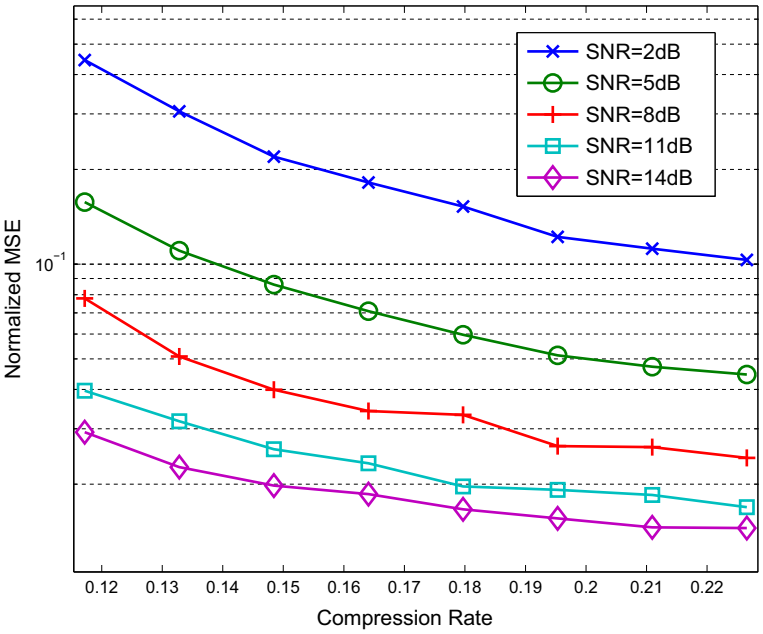

Fig. 5 Estimation performance with different SNR in active band

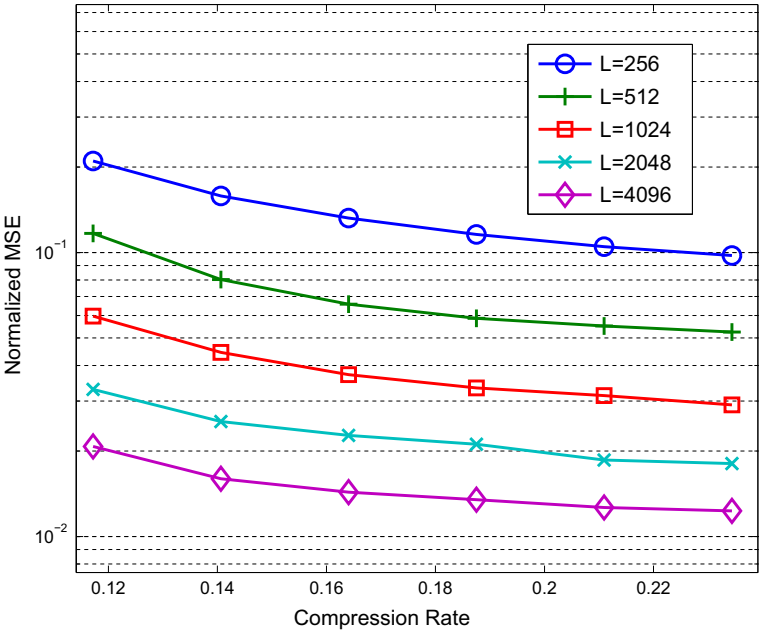

Fig. 6 The NMSE in the active band with different sensing time

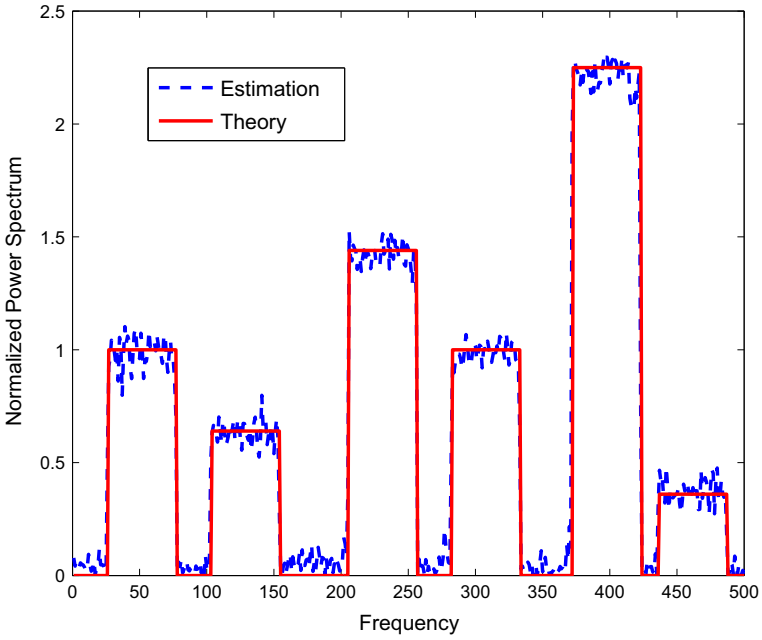

Fig. 7 Power spectrum estimation for less sparse signal. Compression rate is 0.25

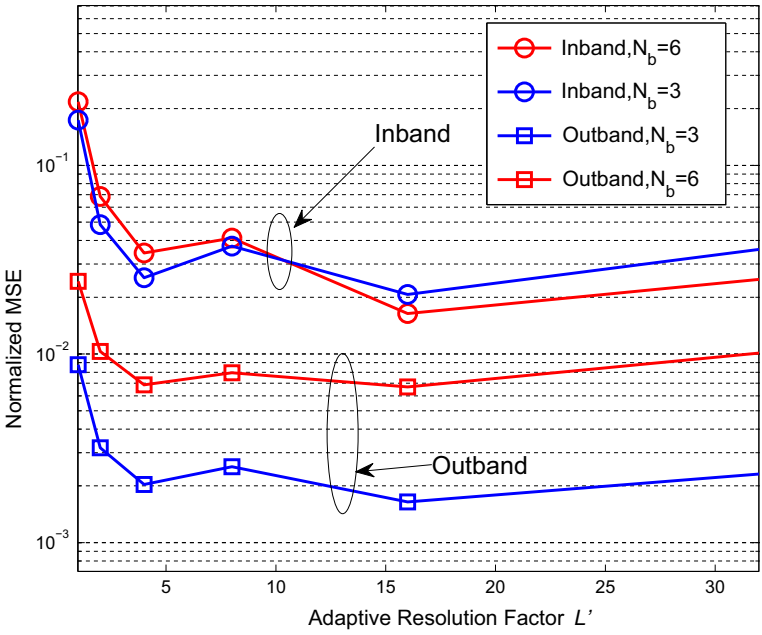

Fig. 8 The NMSE in the active band and the out band with different N_b

$$P_r = \begin{cases} P_x + \delta^2 & \textit{In the active band} \\ \delta^2 & \textit{Out of the active band} \end{cases} \tag{35}$$

where P_x is the theoretical power spectrum of the input and δ^2 is the additive white Gaussian noise power level.

The estimation performance of the active band is analyzed in the following experiments. In Fig. 5, compression rate is M/N, where $N = 128$. The SNR is only calculated in active bands. The number of active bands N_b is 4, and each band employs 40 subcarriers. In Fig. 6, the NMSE in active bands with different sensing times (denoted with L) is illustrated, and SNR = 10 dB.

In Fig. 7, $N = 128$ and compression rate is 0.25. The original signal occupies six subbands. The sparse level is 0.6. The ARFA method is also suitable for less sparse signals. The compression rate can not be less than 0.6 in the spectrum sensing methods based on signal recovery, and such methods are always sensitive to sparsity level. The results in Figs. 5 and 6 also illustrate that the proposed method is not sensitive to sparsity level, because the NMSE does not converge quickly as compression rate increases.

In Fig. 8, $N = 128$, and $M = 32$. The SNR in active bands is 10 dB. The number of active bands N_b are 3 and 6 respectively, and each subband employs 32 subcarriers. The effect of sparsity level on estimation performance in the active band is considerable, but the higher sparsity level leads increases of NMSE out of the active band. The error is mainly resulted from the power leakage from the active subbands. Lower value of L' indicates lower frequency resolution and lower operation complexity; however, when L' is too small, estimation performance degradation results, mainly from the envelope fluctuation.

6 Conclusion

In this study, sub-Nyquist sampling was employed for spectrum sensing in a cognitive radio system, focusing primarily on power spectrum estimation of the wide-sense stationary analog signal. To account for practical implementation, an adaptive resolution frequency averaging (ARFA) scheme was proposed with accepted complexity. The proposed method consists of a set of LS problems with a rank condition for reliable estimation. Compared to other spectrum sensing methods based on sub-Nyquist sampling, this scheme is suitable for both sparse and nonsparse signals. The scheme is easily implemented to detect active subbands with a threshold in CR systems.

References

1. Mitola, J., & Maguire, J. G. Q. (1999). Cognitive radio: Making software radios more personal. *IEEE Personal Communications*, *6*(4), 13–18.
2. Axell, E., Leus, G., Larsson, E., & Poor, H. (2012). Spectrum sensing for cognitive radio: State-of-the-art and recent advances. *IEEE Signal Processing Magazine*, *29*(3), 101–116.
3. Gavrilovska, L., & Atanasovski, V. (2011). Spectrum sensing framework for cognitive radio networks. *Wireless Personal Communications*, *59*(3), 447–469.
4. Candes, E., & Wakin, M. (2008). An introduction to compressive sampling. *IEEE Signal Processing Magazine*, *25*(2), 21–30.
5. Nguyen, V. T., Villain, F., & Le Guillou, Y. (2011). Cognitive radio systems: Overview and challenges. In *2011 3rd International conference on awareness science and technology (iCAST)* (pp. 497–502).

6. Tian, Z., & Giannakis, G. (2007). Compressed sensing for wideband cognitive radios. In *IEEE international conference on acoustics, speech and signal processing, 2007. ICASSP 2007* (Vol. 4, pp. 1357–1360).
7. Wang, Y., Tian, Z., & Feng, C. (2010). A two-step compressed spectrum sensing scheme for wideband cognitive radios. In *2010 IEEE global telecommunications conference (Globecom 2010)* (pp. 1–5).
8. Sun, H., Chiu, W. Y., & Nallanathan, A. (2012). Adaptive compressive spectrum sensing for wideband cognitive radios. *IEEE Communications Letters*, *16*(11), 1812–1815.
9. Sun, H., Chiu, W. Y., Jiang, J., Nallanathan, A., & Poor, H. (2012). Wideband spectrum sensing with sub-Nyquist sampling in cognitive radios. *IEEE Transactions on Signal Processing*, *60*(11), 6068–6073.
10. Jiao, L., Chen, J., Wu, J., Wang, X., & Zhang, S. (2012). Efficient collaborative spectrum sensing with low sample rate. *Wireless Personal Communications*, *67*(4), 923–936.
11. Wang, Y., Tian, Z., & Feng, C. (2012). Sparsity order estimation and its application in compressive spectrum sensing for cognitive radios. *IEEE Transactions on Wireless Communications*, *11*(6), 2116–2125.
12. Mehanna, O., & Sidiropoulos, N. (2013). Frugal sensing: Wideband power spectrum sensing from few bits. *IEEE Transactions on Signal Processing*, *61*(10), 2693–2703.
13. Yen, C. P., Tsai, Y., & Wang, X. (2013). Wideband spectrum sensing based on sub-Nyquist sampling. *IEEE Transactions on Signal Processing*, *61*(12), 3028–3040.
14. Ariananda, D., & Leus, G. (2012). Compressive wideband power spectrum estimation. *IEEE Transactions on Signal Processing*, *60*(9), 4775–4789.
15. Leus, G., & Arianand a, D. (2011). Power spectrum blind sampling. *IEEE Signal Processing Letters*, *18*(8), 443–446.
16. Lexa, M. A., Davies, M., Thompson, J., & Nikolic, J. (2011). Compressive power spectral density estimation. In *2011 IEEE international conference on acoustics, speech and signal processing (ICASSP)* (pp. 3884–3887).
17. Kirolos, S., Ragheb, T., Laska, J., Duarte, M., Massoud, Y., & Baraniuk, R. (2006). Practical issues in implementing analog-to-information converters. In *The 6th international workshop on system-on-chip for real-time applications* (pp. 141–146).
18. Lexa, M. A., Davies, M., & Thompson, J. (2012). Reconciling compressive sampling systems for spectrally sparse continuous-time signals. *IEEE Transactions on Signal Processing*, *60*(1), 155–171.
19. Mishali, M., & Eldar, Y. (2010). From theory to practice: Sub-Nyquist sampling of sparse wideband analog signals. *IEEE Journal of Selected Topics in Signal Processing*, *4*(2), 375–391.
20. Stoica, P., & Moses, R. (2005). *Spectral analysis of signals*. Englewood Cliffs, NJ: Prentice Hall.
21. Batra, A., Lingam, S., Balakrishnan, J. (2006). Multi-band ofdm: A cognitive radio for uwb. In Proceedings of 2006 IEEE international symposium on circuits and systems, 2006. ISCAS 2006 (pp. 4094–4097).
22. Mahmoud, H., Yucek, T., & Arslan, H. (2009). OFDM for cognitive radio: Merits and challenges. *IEEE Wireless Communications*, *16*(2), 6–15.

Lebing Pan received the B.S. degree in communication engineering from Tongji University, Shanghai, China, in 2010 and is currently pursuing the Ph.D. degree in communication and information system at Shanghai Institute of Microsystem and Information Technology, Chinese Academy of Sciences (CAS), Shanghai, China. He is also with the Key Laboratory of Wireless Sensor Networks and Communications, Chinese Academy of Sciences. His research interests include compressive sensing, baseband signal processing, cognitive radio.

Shiliang Xiao received the B.S. degree in electronic and communication engineering from Zhejiang University, Hangzhou, China, in 2010 and is currently pursuing the Ph.D. degree in communication and information system at Shanghai Institute of Microsystem and Information Technology, Chinese Academy of Sciences (CAS), Shanghai, China. He is also with the Key Laboratory of Wireless Sensor Networks and Communications, Chinese Academy of Sciences. His research interests include wireless ad hoc and sensor networks, algorithm design and analysis, and cloud computing.

Xiaobing Yuan received the Ph.D. degree in Changchun Institute of Optics, Fine Mechanics and Physics, Chinese Academy of Science in 2000. He is now a Professor and Ph.D. supervisor in Shanghai Institute of Microsystem and Information Technology, Chinese Academy of Science, Shanghai China. His research interest includes wireless senor network, information transmission and processing.